Elastic scattering of 50 MeV $\pi^{\pm}$ from ^{58}Ni, ^{60}Ni, and ^{64}Ni

C. S. Mishra[(a)*] B. Fick[(b)†] and M. Blecher[(b)] W. Burger[(c)‡] R. L. Burman[(d)] G. Ciangaru[(e)§]
J. Escalante[(a)] K. Gotow[(b)] M. V. Hynes[(d)] B. M. Preedom[(a)]
B. G. Ritchie[(e)**] C. S. Whisnant[(a)] D. H. Wright[(b)]
[(a)]*University of South Carolina, Columbia, South Carolina 29208*
[(b)]*Virginia Polytechnic Institute and State University, Blacksburg, Virginia 24061*
[(c)]*Massachusetts Institute of Technology, Cambridge, Massachusetts 02139*
[(d)]*Los Alamos National Laboratory, Los Alamos, New Mexico 87545*
[(e)]*University of Maryland, College Park, Maryland 20742*
(Received 19 November 1987)

Angular distributions have been measured for $\pi^{\pm}$ elastic scattering at 50 MeV from ^{58}Ni, ^{60}Ni, and ^{64}Ni. A target isospin dependence is observed in the π^+ angular distributions in the region of the diffraction minimum, while the effect is less pronounced for π^-. The π^- angular distributions for these isotopes have a very deep minimum compared with those for π^+. The angular distributions are compared with predictions of the second-order Michigan State University potential. The potential describes the π^+ data much better than the π^- data, though qualitative agreement was obtained for both. The discrepancy between the experimental and calculated cross sections is discussed. The Coulomb distortion of the nuclear amplitude is shown to be important in the region of the diffraction minimum. The π^+/π^- difference introduced by this distortion is responsible for the striking energy dependence of the cross sections near the diffraction minimum between 50 and 80 MeV and can account for the poorer agreement for π^-.

I. INTRODUCTION

A recent study[1] of the neutron density dependence of the pion-nucleus interaction on carbon isotopes at 50 MeV has shown an effect proportional to $(N-Z)/A$, where A, Z, and N are the mass, charge, and neutron numbers, resectively. An optical model analysis of those data using the Michigan State University (MSU) (Refs. 2–4) potential with isoscalar terms proportional to the matter density, $\rho(r)$, and isovector terms proportional to $[(N-Z)/A]\,\rho(r)$, has provided a reasonable description of the angular distributions. To further study this $(N-Z)/A$ dependence, we have extended our studies to a different mass region using the isotopes ^{58}Ni, ^{60}Ni, and ^{64}Ni as targets. The MSU optical potential describes, qualitatively, all of the π^+ angular distributions presented here, but does not describe the π^- angular distributions very well.

II. EXPERIMENTAL PROCEDURE

This experiment was performed at the Clinton P. Anderson Meson Physics Facility (LAMPF) using the low-energy pion (LEP) channel and the Bicentennial Spectrometer (BCS) as discussed in detail in previous publications.[5–7] The π^- scattering cross sections in the diffraction minimum region were measured by the new clamshell spectrometer, described in detail by Fick *et al.*[8] The salient features of the experimental method are briefly reviewed here.

The beam spot was aligned on the target by using an integrating multiwire profile monitor. The beam spot size on the target was 0.3 cm $(V)\times 1.0$ cm (H) FWHM. The momentum resolution was $\Delta P/P=1.0\%$, except at forward angles, where $\Delta P/P=0.5\%$ was used. For the clamshell runs $\Delta P/P=0.7\%$.

The ^{58}Ni ($\rho t=0.146$ g/cm^2), ^{60}Ni ($\rho t=0.150$ g/cm^2), and ^{64}Ni ($\rho t=0.145$ g/cm^2) targets were self-supporting foils. For the BCS measurements the background was found to be negligible for all targets and an energy resolution of $\lesssim 1.0$ MeV FWHM was achieved. This resolution was sufficient to separate elastic form inelastic scattering. The data in the diffraction minimum region for π^- scattering were taken with the clamshell spectrometer. A vacuum scattering chamber for this measurement was not available, and scattering from air required background measurements at each angle even though an energy resolution of 650 keV was achieved. The yields for these angles are the differences of target in minus target out, and the statistical errors for the two runs were combined in quadrature. These are the errors given in Table II (90°–105°). The error introduced by the background subtraction is about 10%.

The relative normalization was determined with a pion decay monitor telescope[9] placed at an angle with respect to the beam which was small compared with the muon opening angle. This setting kept the monitor insensitive to minor shifts in beam centroid.

During the BCS runs absolute normalization of the (π^+,π^+) cross section was determined by measuring π^+p and $\pi^+\,^{12}$C elastic scattering from a CH_2 target ($\rho t=0.236$ g/cm^2) at 55°, 75°, 95°, 105°, and 115°. The cross sections were normalized to both the data of Bertin[10] *et al.* for π^+p scattering and to that of Preedom[11] *et al.* for $\pi^+\,^{12}$C scattering. The two normalizations agreed within statistical uncertainties. The absolute normalization of the (π^-,π^-) cross sections was determined by $\pi^-\,^{12}$C elastic scattering from a CH_2 target and normalized to the $\pi^-\,^{12}$C measurement of Sobie *et al.*[12] at 50

MeV. The normalization uncertainties achieved were $\pm 6.2\%$ for π^+ and $\pm 9.5\%$ for π^-. These errors include statistical and systematic errors in both the present measurement and the published cross sections used as reference.

III. RESULTS AND ANALYSIS

The ^{58}Ni, ^{60}Ni, and ^{64}Ni π^+ elastic scattering differential cross sections are listed in Table I and shown in Fig. 1. Those for π^- scattering are listed in Table II and shown in Fig. 2. There is a small systematic difference between the three nickel isotopes. The angular distributions for π^+ scattering have a shallow diffraction minimum at $\sim 105°$, with the cross sections in that region decreasing with increasing neutron number. The angular distributions for π^- scattering have much deeper diffraction minima than for π^+ scattering. For π^+ the isotopic dependence of the cross sections in the region of the diffraction minimum is quite apparent. For π^- scattering, however, isospin effects are not so clear, but the minimum appears to deepen as the neutron number decreases. Smaller isospin differences are observed for the nickel isotopes than were observed for the carbon isotopes,[1,13] in agreement with the $(N-Z)/A$ dependence of the isospin terms in the pion-nucleus interaction as described later.

Optical model calculations using the second-order MSU optical potential [Eq. (1) of Ref. 4] were performed for all of the angular distributions presented in Figs. 1 and 2 using the code MSUPIRK. The MSU potential includes both isoscalar and isovector interactions with terms proportional to the square of the nuclear density. The isoscalar terms depend on the nuclear density and the isovector terms are proportional to the neutron-proton density difference. This density difference is approximated by $\rho(r)(N-Z)/A$.

The nuclear matter density, assumed to have the same shape for neutrons and protons, was taken to be the Woods-Saxon form

$$\rho(r)=\frac{\rho_0}{1+e^{(r-c)/A}} .$$

The charge distribution was approximated by a uniform distribution. The mass and charge density parameters were taken from compilations of the electromagnetic measurements.[14] The parameters used here were (a) ^{58}Ni, $c=4.08$ fm, $a=0.56$ fm; (b) ^{60}Ni, $c=4.15$ fm, $a=0.58$ fm; and (c) ^{64}Ni, $c=4.21$ fm, $a=0.58$ fm.

The MSU optical potential parameters were taken to be the published values (set E) (Ref. 4) calculated from pion-nucleon scattering amplitudes, fits to pionic atom data, and a global fit to other 50 MeV π^+ nucleus elastic scattering data. The agreement between the calculations and the experimental distributions is reasonably good for all of the π^+ angular distributions as shown in Figs. 3–5, and correctly describes the isotope effect observed at the diffraction minimum. For π^- the calculations overestimate the cross sections in the s-p wave interference region (45°–65°) and in the diffraction minimum region (95°). The same behavior was noted for the nickel isotopes at 65 MeV and at 50 MeV (Ref. 12) for ^{12}C. The χ^2 per point is approximately 20 for each π^+ angular distribution and greater than 200 for each π^- angular distribution (see Table III). Good fits to the data may be obtained by varying the model parameters. Adjusting the optical potential and/or the density parameters to reproduce the data presented here cannot be justified, since the physical meaning of the varied parameter is not at all obvious. One can draw conclusions from such variations only if all the existing π^+ and π^- data are included in a global fit, as done by the MSU group. Such a global analysis, in-

TABLE I. Elastic differential cross section for ^{58}Ni$(\pi^+,\pi^+)^{58}$Ni, ^{60}Ni$(\pi^+,\pi^+)^{60}$Ni, and ^{64}Ni$(\pi^+,\pi^+)^{64}$Ni. Scattering angle and cross sections are in the center of mass (c.m.) with units of degrees and mb/sr, respectively.

Target	$\theta_{\text{c.m.}}$	$(d\sigma/d\Omega)_{\text{c.m.}}$ (mb/sr)	$\Delta\sigma^{a}_{\text{c.m.}}$ (mb/sr)
^{58}Ni	20.1	309.0	28.0
	30.1	125.0	4.0
	40.1	64.2	2.0
	50.2	29.1	0.8
	55.2	21.9	0.6
	60.2	19.0	0.5
	70.2	14.4	0.4
	75.2	13.8	0.3
	80.2	12.0	0.3
	90.2	7.10	0.41
	95.2	5.11	0.30
	100.2	4.04	0.26
	105.2	3.10	0.22
	110.2	3.72	0.28
	115.2	4.59	0.30
^{60}Ni	20.1	284.0	26.0
	30.1	124.0	3.1
	40.1	58.4	1.9
	50.1	27.8	0.7
	55.2	19.8	0.5
	60.2	15.7	0.4
	70.2	14.6	0.4
	75.2	12.7	0.4
	80.2	9.73	0.27
	90.2	5.53	0.23
	95.2	4.34	0.19
	105.2	2.58	0.14
	115.2	3.63	0.20
^{64}Ni	20.1	286.0	27.0
	30.1	131.0	3.7
	40.1	64.4	2.0
	50.1	27.0	0.7
	55.1	18.3	0.5
	60.2	15.6	0.4
	70.2	11.6	0.3
	75.2	10.3	0.3
	80.2	9.19	0.25
	90.2	4.74	0.30
	95.2	3.00	0.16
	105.2	2.13	0.13
	115.2	2.85	0.10

[a]The errors shown are due to statistics. The normalization error is 6.2% for π^+.

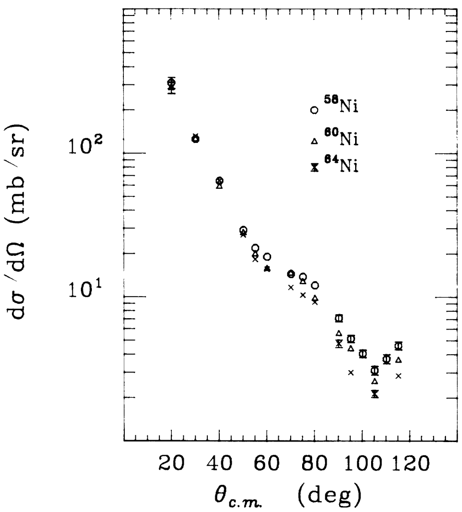

FIG. 1. Elastic differential cross sections for π^+ scattering on ^{58}Ni, ^{60}Ni, and ^{64}Ni at 50 MeV.

cluding this data as well as all other existing π^+ and π^- elastic, inelastic, and single and double charge exchange data for pion energies below 100 MeV, is in progress by another group.[15]

The difference between the calculations and the data reflect the fact that only π^+ nucleus scattering data were used in the MSU parametrization. In that analysis, the isoscalar part of the hadronic interaction was determined both by theoretical considerations and the π^+ scattering data from $T=0$ nuclei. If the form of the potential is correct, one naively expects that this part of the nuclear interaction could be determined equally well from either π^+ or π^- data. With the isoscalar interaction fixed, the addition of the isovector terms should produce changes to the cross sections that are both small and symmetric since these terms add for π^- and subtract for π^+. For ^{58}Ni, where the isovector terms are smallest, the discrepancy between the calculation and the data for π^- appears to be much larger than the estimated uncertainties in the isovector strengths. The difference in the quality of agreement for π^+ and π^- indicates that this simple analysis is inadequate. The Coulomb distortions of the nuclear amplitudes are not the same for the two pion charge and are responsible for the observed π^+/π^- differences. In the presence of these distortions the information obtained by scattering π^+ or π^- is thus complementary. To understand how these data complement each other, the effects of the Coulomb distortions are examined in greater detail.

To illustrate the nature of these distortions, an analysis of the energy dependence of the nuclear and Coulomb amplitudes has been performed for ^{58}Ni using an energy- and mass-dependent, phenomenological optical potential. This potential is a zero-range Kisslinger potential which includes the angle transformation term. The correspondence between this potential and the MSU parametrization has been discussed in detail by Seki and Masutani.[16] The parameters in this model were adjusted to reproduce elastic scattering data throughout the periodic table for

TABLE II. Elastic differential cross section for ^{58}Ni(π^-, π^-)^{58}Ni, ^{60}Ni(π^-,π^-)^{60}Ni, and ^{64}Ni(π^-,π^-)^{64}Ni. Scattering angle and cross sections are in the center of mass (c.m.) with units of degrees and mb/sr, respectively.

Target	$\theta_{c.m.}$	$(d\sigma/d\Omega)_{c.m.}$ (mb/sr)	$\Delta\sigma^{a}_{c.m.}$ (mb/sr)
^{58}Ni	20.1	1021.0	62.0
	30.1	339.0	13.0
	40.1	104.0	3.9
	50.2	44.1	1.2
	60.2	32.4	0.9
	70.2	23.9	0.7
	80.2	11.2	0.4
	82.7	7.93	0.60
	85.0	4.30	0.31
	85.2	4.00	0.40
	87.3	3.60	0.70
	90.2	1.77	0.19
	93.9	0.34	0.12
	96.2	0.13	0.10
	98.5	0.31	0.12
	98.9	0.92	0.20
	101.2	1.10	0.21
	103.5	1.20	0.30
	105.2	2.92	0.18
	115.2	6.47	0.52
^{60}Ni	20.1	1119.0	60.0
	30.1	346.0	13.0
	40.1	107.0	4.3
	50.1	47.0	1.4
	60.2	34.9	1.2
	70.2	24.3	0.7
	80.2	10.6	0.3
	90.2	1.42	0.20
	105.2	3.40	0.15
	115.2	6.84	0.25
^{64}Ni	20.1	1159.0	66.0
	30.1	377.0	15.0
	40.1	108.0	4.2
	50.1	48.9	1.3
	60.2	34.9	1.0
	70.2	24.8	0.7
	80.2	8.32	0.36
	82.7	7.50	1.20
	85.0	4.50	0.50
	87.3	1.30	0.30
	90.2	1.07	0.14
	93.9	0.56	0.18
	96.2	0.38	0.13
	98.5	0.60	0.17
	98.9	1.60	0.30
	101.2	2.00	0.30
	103.5	3.80	0.80
	105.2	3.91	0.12
	115.2	6.63	0.22

[a]The errors shown are due to statistics. The normalization error is 9.5% for π^-.

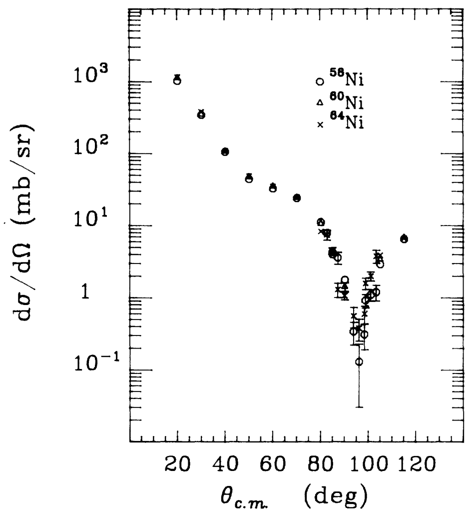

FIG. 2. Elastic differential cross sections for π^- scattering on ^{58}Ni, ^{60}Ni, and ^{64}Ni at 50 MeV.

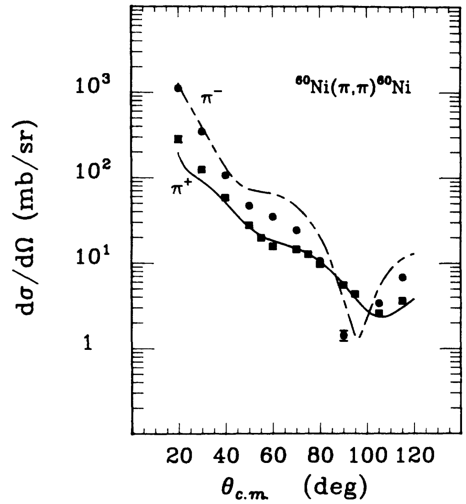

FIG. 4. Elastic differential cross section for ^{60}Ni($\pi^{\pm}$, $\pi^{\pm}$)^{60}Ni. The curves are calculations with the MSU optical potential, as discussed in the text.

pion energies between 15 and 100 MeV. Further details of this potential and the fitting procedure are described in Ref. 17. This potential contains only four parameters and is well constrained by the fitting procedure. Thus, it is a useful tool for examining systematic trends in the data.

Since the π^+/π^- difference is most dramatic in the diffraction minimum, the model analysis was performed for a momentum transfer of 0.916 fm^{-1}, corresponding to 90° and 50 MeV. Near the diffraction minimum, which results, in part, from cancellations between the nuclear and Coulomb amplitudes, the cross sections are sensitive to the relative phases and magnitudes of these amplitudes. Specifically, the differences between the minima for π^+ and π^- are expected to depend on the phase and magnitude of the Coulomb distorted nuclear amplitude (F_n) with respect to the Coulomb amplitude (F_c). To represent these as a function of energy, Fig. 6 shows a plot of the phase angle between the nuclear and Coulomb amplitudes, ϕ_{nc}, vs the ratio of the magnitudes, F_n/F_c, for energies between 40 and 80 MeV. The very different energy dependences for π^+ and π^- illustrate the strong distortions of the nuclear amplitudes at this momentum transfer. From the figure, variations in the relative magnitudes of the π^+ and π^- cross sections may be inferred. Below 50 MeV, the nuclear and Coulomb amplitudes are almost equal for π^- and π^+, but the relative phase is $\sim 180°$ for π^- whereas it is $\lesssim 80°$ for π^+. As the energy increases, the π^+ nuclear amplitude changes very little relative to the Coulomb, while ϕ_{nc} increases. This results in a more complete cancellation, lowering the cross section. The π^- nuclear amplitude changes very little in phase relative to the Coulomb, but increases in magnitude, increasing the cross section. Thus, it is the increase

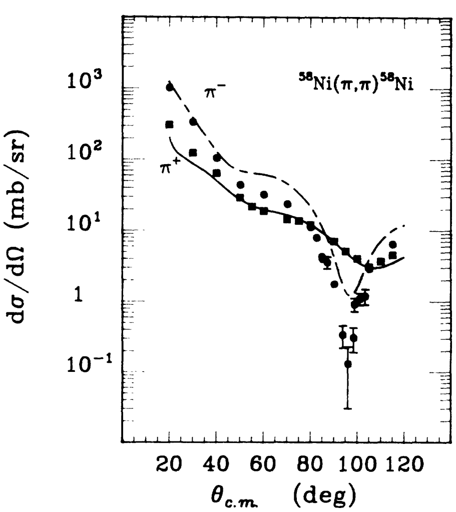

FIG. 3. Elastic differential cross section for ^{58}Ni($\pi^{\pm}$, $\pi^{\pm}$)^{58}Ni. The curves are calculations with the MSU optical potential, as discussed in the text.

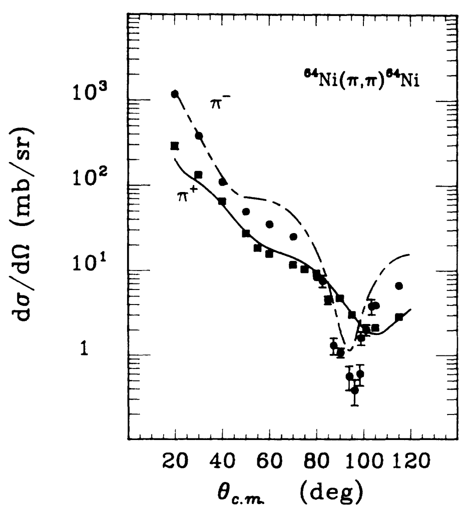

FIG. 5. Elastic differential cross section for ^{64}Ni($\pi^{\pm}$, $\pi^{\pm}$)^{64}Ni. The curves are calculations with the MSU optical potential, as discussed in the text.

in ϕ_{nc} for π^+ and the increase in F_n/F_c for π^- which determines the energy dependence. This energy dependence for the Coulomb distorted nuclear amplitudes can account for both the observed π^+/π^- difference seen in the diffraction minimum here at 50 MeV and the quite different result seen at 65 MeV (Ref. 8) where the π^+ diffraction minimum is deeper than the π^-. At 80 MeV this reversal is complete, with π^+ much deeper than π^-. For ^{40}Ca, where there are published data available for 50, 65, and 80 MeV (Refs. 11, 18, and 19, respectively), the same behavior is observed.

In the optical model used for these calculations, there are only four parameters: the real and imaginary s- and p-wave interaction strengths; the same parameters are used for both the π^+ and π^- calculations. The difference between the Coulomb distorted nuclear amplitudes for the two pion charges is due to simply changing the sign of the charge in the Coulomb interaction. In the absence of the Coulomb distortions of the nuclear amplitudes, F_n/F_c would be equal for π^+ and π^- using this isoscalar optical potential and the two ϕ_{nc} would differ by approximately 180°. As seen in Fig. 6, this is clearly not the case in the presence of the Coulomb field. The pure nuclear amplitude is modified by the Coulomb interaction in a different way for π^+ and π^-, effectively giving different potentials for the two cases. Including isovector terms in the potential will also produce different nuclear amplitudes for π^+ and π^-. These isovector-term differences, however, cannot account for the observed π^+/π^- energy dependence in the diffraction minimum in the ^{40}Ca data where $T=0$. Nor should their presence substantially change the effects of the Coulomb distortions for the $(T\neq 0)$ nickel isotopes. The isovector effects are much too small as evidenced by the small isotopic differences seen for a given pion charge.

The qualitative behavior of the four parameters in the potential is given in Ref. 17. Over the energy range of 50–80 MeV, the imaginary s-wave and real p-wave strength are changing by a few percent or less. But in this same energy range as resonance is approached, the imaginary p-wave strength more than doubles and the real s-wave strength decreases by about 30%. It is essentially the change in these two parameters which is producing the observed energy dependence.

The sensitivity to the parameters used in the phenomenological optical model was checked by varying, separately, each of the parameters by 10%. These variations made only minor changes in the amplitudes and phases and have no effect on the conclusions presented earlier. A comparison was also made to MSU calculations at 40, 50, and 65 MeV. The 40 MeV parameters were interpolated from set E of Ref. 4, and the 65 MeV calculation is described in Ref. 8. Since the MSU and phenomenological potentials do not produce exactly the same cross sections near the diffraction minimum, the amplitude and phase are numerically different. However, the trend with energy is the same for both calculations. The MSU calculations confirm that the increase in ϕ_{nc} for π^+ and the increases in F_n/F_c for π^-, produce the observed energy dependence.

Because the MSU analysis[2–4] did not include π^- data or extend to energies between 50 and 100 MeV for π^+, no data which included a strong cancellation in the diffraction minimum were included in that study. In π^- scattering at 50 MeV, and both π^+ and π^- scattering at the higher energies, the cancellation between the Coulomb and nuclear amplitudes makes the calculated cross sections much more sensitive to the individual s- and p-wave parts of the interaction than for π^+ at the lower energies where the amplitudes essentially add. Coulomb-nuclear interference effects have been examined previously in low-energy pion scattering at angles less than 30° (Ref. 20). At small angles where the Coulomb and nuclear amplitudes are the same magnitude, differences between π^+ and π^- data are dominated by the different relative Coulomb-nuclear phases. The present analysis explicitly shows that the Coulomb and nuclear amplitudes are still comparable near 90°. In the diffraction minimum, the Coulomb distortions of the nuclear amplitude are responsible for the observed energy dependence. It is precisely in this angular range that the

TABLE III. χ^2 per point for different reactions using the set E (Ref. 4) parameters of the MSU potential as discussed in the text.

Reaction	χ^2/pt
^{58}Ni(π^+,π^+)	19
^{58}Ni(π^-,π^-)	211
^{60}Ni(π^+,π^+)	18
^{60}Ni(π^-,π^-)	295
^{64}Ni(π^+,π^+)	22
^{64}Ni(π^-,π^-)	236

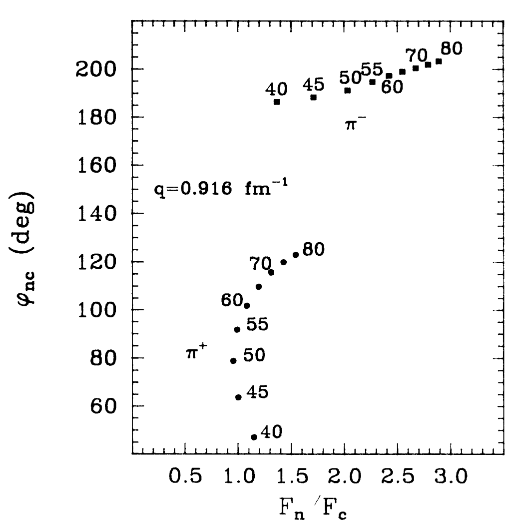

FIG. 6. The phase angle between the nuclear and Coulomb amplitudes, ϕ_{nc}, is shown versus the ratio of the magnitudes of the nuclear to Coulomb amplitudes, F_n/F_c for ^{58}Ni. The calculations are done for a momentum transfer of 0.916 fm^{-1}, corresponding to 90° at 50 MeV. The squares represent the π^- and the circles π^+. Calculations were done every 5 MeV and the points are labeled by the incident pion energy in MeV.

data exhibit the largest dependence on the isovector part of the interaction. Because the Coulomb interaction, which does not preserve the isospin symmetry, has such a dominant effect in this angular region, extraction of reliable isovector densities and potential parameters is difficult. Only by including these data with other, high quality data, from a variety of nuclei at energies between 50 and 100 MeV in a systematic and detailed analysis, can one hope to extract this information.

IV. CONCLUSION

An isospin dependence of the $\pi^{\pm}$ elastic scattering has been observed by comparing ^{58}Ni, ^{60}Ni, and ^{64}Ni differential cross sections at 50 MeV. The MSU optical potential qualitatively describes the angular distributions indicating that the neutron density distribution is given approximately by $[(N-Z)/A]\ \rho_p(r)$. However, in the angular range where the isospin effects are largest, Coulomb-nuclear interference and Coulomb distortion of the nuclear amplitude are shown to be important. The extraction of reliable isovector densities requires not only a relativistic optical potential with a well-determined isoscalar component, but also a careful treatment of the Coulomb interaction. This can only be done by making a consistent analysis of data from a variety of nuclei over a wide range of energies. The data presented here should aid in achieving this goal.

ACKNOWLEDGMENTS

The authors would like to thank the staff of LAMPF for their support during the experiments. We would also like to thank J. A. Carr, K. Stricker-Bauer, and H. McManus for providing us with their optical model code. This work was supported by the National Science Foundation (University of South Carolina, VPI and SU, and the University of Maryland) and by the Department of Energy (LANL, MIT).

*Present address: Physics Division, P-2, MS D456, Los Alamos National Laboratory, Los Alamos, NM 87545.
†Present address: University of Utah, Salt Lake City, Utah 84112.
‡Present address: Swiss Institute for Nuclear Physics, CH-5234, Villigen, Switzerland.
§Present address: P.O. Box 2175, Schlumberger Well Service, 5000 Gulf Hwy., Houston, TX 77252.
**Present address: Arizona State University, Tempe, AZ 85281.
[1] C. S. Mishra *et al.*, Phys. Rev. C **32**, 995 (1985).
[2] K. Stricker, H. McManus, and J. A. Carr, Phys. Rev. C **19**, 929 (1979).
[3] K. Stricker, J. A. Carr, and H. McManus, Phys. Rev. C **20**, 2043 (1980).
[4] J. A. Carr, H. McManus, and K. Stricker-Bauer, Phys. Rev. C **25**, 952 (1982).
[5] M. J. Leitch *et al.*, Phys. Rev. C **29**, 561 (1984).
[6] M. Blecher *et al.*, Phys. Rev. C **25**, 2554 (1982).
[7] C. S. Mishra, M.S. thesis, University of South Carolina, 1982 (unpublished).
[8] B. Fick *et al.*, Phys. Rev. C **34**, 643 (1986).
[9] E. A. Wadlinger, Nucl. Instrum. Methods **134**, 243 (1976).
[10] P. Y. Bertin, Nucl. Phys. **B106**, 341 (1976).
[11] B. M. Preedom *et al.*, Phys. Rev. C **23**, 1134 (1981).
[12] R. J. Sobie *et al.*, Phys. Rev. C **30**, 1612 (1984).
[13] M. Blecher *et al.*, Phys. Rev. C **28**, 2033 (1983).
[14] C. W. DeJager, H. DeVries, and C. DeVries, At. Data Nucl. Data Tables **14**, 479 (1974); H. DeVries, C. W. DeJager, and C. DeVries, At. Data Nucl. Data Tables **36**, 495 (1987).
[15] P. Alons and E. Siciliano, private communication.
[16] Seki and Masutani, Phys. Rev. C **27**, 2799 (1983).
[17] C. S. Whisnant, Phys. Rev. C **34**, 262 (1986).
[18] S. Dam *et al.*, Phys. Rev. C **25**, 2574 (1982).
[19] M. J. Leitch *et al.*, Phys. Rev. C **29**, 561 (1982).
[20] H. Degitz *et al.*, Phys. Lett. **141B**, 41 (1984).